Decay of Radioactive Ce¹⁴³ (33.4 hr)*

D. W. Martin, M. K. Brice,† J. M. Cork,† and S. B. Burson
Argonne National Laboratory, Lemont, Illinois
(Received September 19, 1955)

The beta and gamma radiations of Ce¹⁴³ have been studied with a ten-channel scintillation coincidence spectrometer, with a double-focusing magnetic spectrometer, and with photographic magnetic spectrographs. Five beta-ray components and ten gamma rays are identified with the activity, and the decay scheme is established involving six excited states of the daughter Pr¹⁴³ nucleus. It is found that no beta rays of measurable intensity proceed directly to the Pr¹⁴³ ground state. Spin and parity assignments are made for several of the levels.

I. INTRODUCTION

THE 33-hr beta emitter in cerium was first observed by Pool and Kurbatov.[1] Their assignment of the activity to Ce¹⁴³ has been confirmed.[2] Several investigations[3-5] of the conversion- and secondary-electron spectra have been in essential agreement on the existence of gamma rays with energies of about 0.057, 0.29, 0.35, 0.66, and 0.72 Mev. Coincident gamma rays of 0.126 and ~0.16 Mev, for which the 0.29-Mev transition was presumed to be the crossover, were suggested[5] from an early scintillation measurement. Beta-ray components of 1.38, 1.09, and 0.71 Mev, with possible others of lower energy, have been reported.[4,5] Each of these investigators has proposed an essentially different level scheme. In particular, two of them have assumed that the highest energy beta ray proceeds to the ground state of Pr¹⁴³.

The gamma-ray spectrum has been studied with the ten-channel scintillation coincidence spectrometer at the Argonne Laboratory, using cubical crystals of NaI(Tl) about 2¼ in. on a side and Dumont 6292 photomultipliers. The internal-conversion electron spectrum has been observed with photographic magnetic spectrographs both at Argonne and at the University of Michigan. The beta-ray spectrum has been analyzed with the double-focusing magnetic spectrometer at the University of Michigan. In addition, the beta-ray spectra in coincidence with various gamma rays have been observed with the scintillation spectrometer, using an anthracene crystal and an RCA 5819 photomultiplier.

Sources were prepared by neutron irradiation of cerium oxide enriched in mass 142 in the Argonne reactor, CP-5. A number of different irradiations ranging up to 37 hours were performed.

II. GAMMA-RAY SPECTRUM

Figure 1 shows the NaI(Tl) pulse-height distribution obtained with a freshly irradiated source in "good"

geometry. As shown in the insert, a lead collimator 4 inches long is used, having a tapered aperture that defines a cone limited to the central part of the crystal. A 1-cm thick slab of Lucite in front of the crystal serves to absorb all beta rays and conversion electrons. The whole assembly is enclosed in a 2-inch thick lead shield. The superimposed Cs¹³⁷ spectrum illustrates the spectrum of a single gamma ray in this geometry.

The decay of the spectrum was observed in this geometry over a period of 12 days. All of the peaks were found to decay with the 33-hr period except for the initially small peak at 0.145 Mev and part of the x-ray peak. These can be attributed to the well-known[6] single gamma ray of Ce¹⁴¹ (33.1-day).

Evident in the figure are "photopeaks" for five of the previously reported gamma rays, as well as several additional peaks. The peak at 0.493 Mev is seen, by comparison with the superimposed Cs¹³⁷ spectrum, to be much too sharp to be due to the Compton distributions of higher energy gamma rays. This and the peaks labeled 0.232 and 0.861 Mev are confirmed to be gamma rays by observation of their conversion lines. The last peak, at 1.10 Mev is not at the right energy for any expected "sum peak" (very unlikely in this geometry), and therefore represents another gamma ray. One additional weak gamma ray at 0.565 Mev will be shown to exist in the discussion of coincidence spectra. No evidence is found for gamma rays of 0.126 or 0.16 Mev.

The gamma rays are listed in Table I together with their associated conversion-electron lines where observed. The energy values quoted are based on the conversion data in most cases. In no case is this value in conflict with the scintillation data. The scintillation spectrometer is calibrated, for the two gamma rays not observed in conversion spectra, with the gamma rays of Cs¹³⁷ and Co⁶⁰. No definite evidence is found in the conversion spectra for any transition not observed by scintillation.

A photometric measurement from the spectrograph plates of the K/L ratio proved to be feasible only for the 0.294-Mev transition, for which the value 6.1±0.6 is obtained. The lines associated with the 0.0574-Mev

[1] M. L. Pool and J. D. Kurbatov, Phys. Rev. **63**, 463 (1943).
[2] M. L. Pool and N. L. Krisberg, Phys. Rev. **73**, 1035 (1948).
[3] H. B. Keller and J. M. Cork, Phys. Rev. **84**, 1079 (1951).
[4] E. Kondaiah, Phys. Rev. **83**, 471 (1951).
[5] W. H. Burgus, Phys. Rev. **88**, 1129 (1952).

[6] Hollander, Perlman, and Seaborg, Revs. Modern Phys. **25**, 469 (1953).
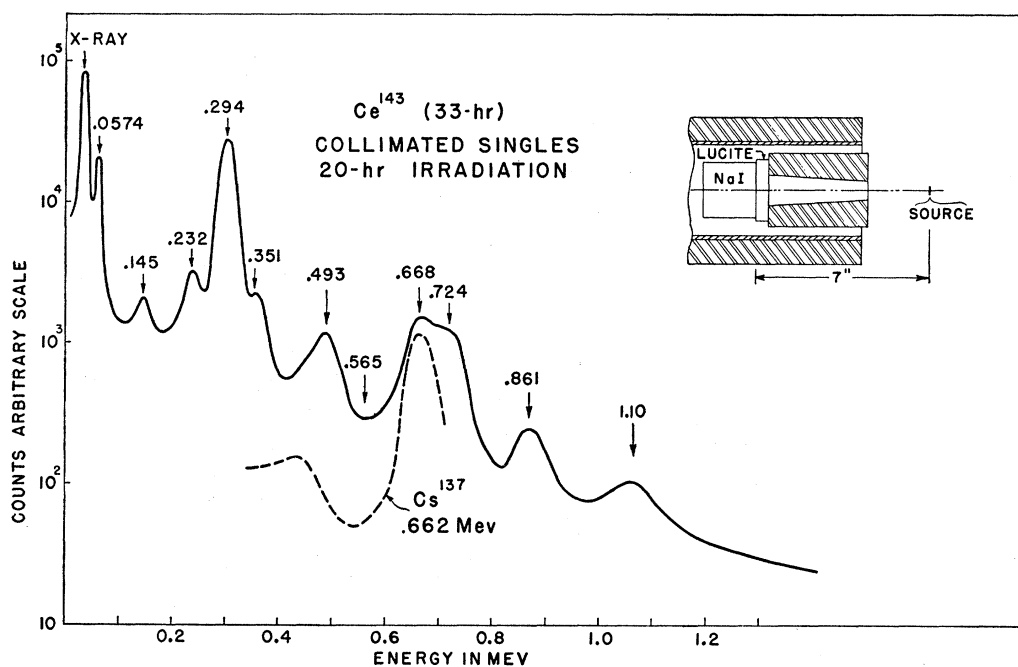
FIG. 1. NaI(Tl) normal pulse-height distribution of Ce^{143} (33.4-hr) in "good" geometry. The geometrical arrangement is illustrated in the insert. The dashed curve is a portion of the pulse distribution of the single gamma ray (0.662 Mev) of Cs^{137} in the same geometry.

transition are actually very intense, but the sensitivity of the photographic emulsion varies rapidly with energy at low energies and causes some uncertainty. Estimates of the K/L ratio led to interpretations in conflict with

TABLE I. Gamma-ray and conversion-line energies in Mev.

Gamma energy	Conversion-line energy	Interpretation	Energy sum
0.0574±0.0002	0.0154	K	0.0574
	0.0505	L_I	0.0575
	0.0560	M	0.0574
	0.0572	N	0.0576
0.1416±0.0003	0.1036	K	0.1416
(Ce^{141})	0.1391	L_{II}	0.1415
0.232 ±0.001	0.1900	K	0.2320
	0.2245	L_I	0.2314
0.294 ±0.001	0.2522	K	0.2942
	0.287	L	0.294
	0.293	M	0.294
0.351 ±0.001	0.309	K	0.351
0.493 ±0.002	0.451	K	0.493
	0.48	L	0.49
0.565 ±0.005	None		
0.668 ±0.002	0.626	K	0.668
0.722 ±0.002	0.682	K	0.722
0.861 ±0.005	0.819	K	0.861
1.10 ±0.01	None		

other data. Only a single rather well-defined L-line is observed for the 0.0574-Mev transition, even though M- and N-lines are readily seen, and it appears definitely to be the L_I subshell line. The implications of this fact for interpretation of the transition character will be shown to be consistent with other data.

For the gamma-gamma coincidence experiments, the source was placed between two identical NaI crystals, which were about $\frac{1}{2}$ inch apart. 900 mg/cm^2 of Al was placed in front of each counter to absorb the beta rays. Pulses from one of the counters were selected with a single-channel differential analyzer and used to gate the ten-channel analyzer. As no "fast" coincidence channel was employed, the coincidence resolving time was 2×10^{-6} second. Rather low counting rates were used, however, so that random coincidences were always negligible. In certain of the experiments, where one counter was observing low-energy events, and the other high-energy events, 4 g/cm^2 of lead was placed in front of the high-energy counter to intercept low-energy quanta scattering back to the low-energy counter.

Curve B in Fig. 2 shows the spectrum of coincidence pulses observed when the gating channel was set on the 0.0574-Mev peak. Curve A is the ungated spectrum for the same geometry, and Curve C is the difference between A and B for energies greater than 0.1 Mev. The situation of the 0.0574-Mev peak in the total spectrum (see Curve A) is such that the gating channel is often actuated by pulses from the intense Pr x-ray peak at 0.036 Mev. These x-rays arise from internal conversion of all of the various gamma rays, and could therefore
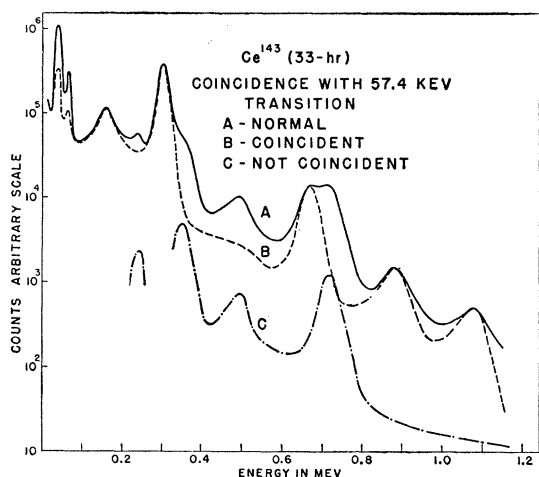
FIG. 2. NaI(Tl) pulse-height distributions of Ce[143] in coincidence geometry (see text). *A*. Ungated spectrum. *B*. Coincidence spectrum gated by the 0.0574-Mev peak. *C*. Difference between *A* and *B*.

give rise to peaks in the coincidence spectrum that are not in coincidence with the 0.0574-Mev transition. This is undoubtedly the explanation for the x-ray and 0.0574-Mev peaks in the coincidence spectrum. However, it is found in other experiments (see below) that, of all the appreciably converted strong transitions (other than the 0.0574-Mev transition itself), none is strongly coincident with anything of energy greater than 0.1 Mev. Thus, virtually all coincidence pulses above this energy must really be coincident with either the gamma quantum or the conversion x-ray of a 0.0574-Mev transition.

To verify these suppositions, the coincidence spectrum was observed with the gating channel moved from the 0.0574-Mev peak to the x-ray peak. As expected, no changes were apparent in the region above 0.1 Mev.
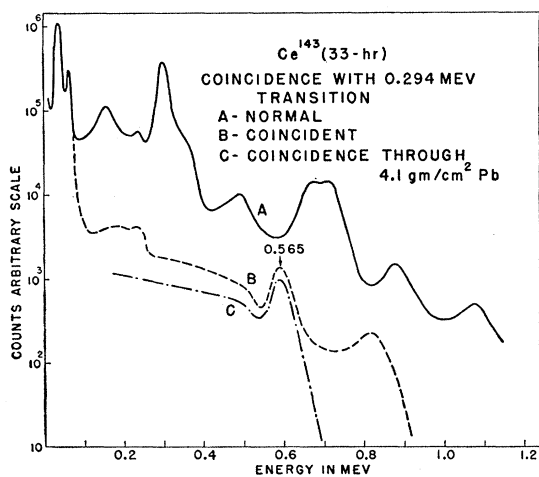

FIG. 3. NaI(Tl) pulse-height distributions of Ce[143] in coincidence geometry (see text). *A*. Ungated spectrum. *B*. Coincidence spectrum gated by the 0.294-Mev peak. *C*. Same as *B*, through 4.1 g/cm² of Pb.

The spectra of Fig. 2 suggest that there exists a low-lying state at 0.0574 Mev in the Pr[143] nucleus, to which all gamma rays in the decay lead except the four of energies 0.232, 0.351, 0.493, and 0.722 Mev. Of these, the 0.351- and 0.722-Mev gamma rays appear from their energies to be crossovers for 0.294–0.0574 and 0.681–0.0574 cascades, respectively. These assumptions are consistent with all other data.

Curve *B* in Fig. 3 is the spectrum of pulses in coincidence with the 0.294-Mev peak. To determine whether the peaks at 0.565 and 0.81 Mev are gamma rays or merely represent Compton scattering of higher energy gamma rays coincident with backscattered quanta of 0.29 Mev, various thicknesses of Pb were placed in front of the counter. The 0.565-Mev coincidence peak was attenuated by amounts characteristic of about 0.55 Mev and therefore represents a gamma ray, while the 0.81-Mev peak showed attenuations appropriate to 0.3 Mev and is thus due to backscattering. The upper portion of the spectrum as it appears through 4.1 g/cm² of Pb is shown as Curve *C* in Fig. 3.

TABLE II. Summary of gamma-gamma coincidence data. *X*: Coincidences observed; 0: coincidences not observed.

| | Gamma-ray energy in Mev | | | | | | | | |
	1.10	0.861	0.722	0.668	0.565	0.493	0.351	0.294	0.232
0.0574	X	X	0	X	?	0	0	X	0
0.232	0	0	0	0	...	X	...	0	
0.294	0	0	0	0	X	0	0		
0.351	0	0	0	0	...	...			
0.493	0	0	0	0	...				
0.565	0	0	0	0					
0.668	0	0	0						
0.722	0	0							
0.861	0								

(Row labels at left: Gamma-ray energy in Mev)

Virtually all x-rays coincident with the 0.294-Mev peak must arise from internal conversion of the 0.0574-Mev transition. Therefore, comparison of the areas of the x-ray and 0.0574-Mev peaks in this coincidence spectrum provides a direct measurement of the K-shell internal-conversion coefficient of the latter transition. The absorption efficiency of the crystal is 100% for both peaks, but corrections must be made for the fluorescent yield of Pr, the relative fractions of iodine K x-ray escapes, and the relative attenuations by beta absorbers and light shields. The value obtained is $\alpha_K = 5.9$, with an estimated uncertainty of less than ten percent.

In further experiments, the 0.232- and 0.493-Mev peaks are found to be in coincidence. None of the four peaks above 0.6 Mev are observed in a coincidence distribution in which the gating channel is set to accept all pulses corresponding to energies above 0.1 Mev. Table II summarizes the gamma-gamma coincidence data. An X indicates that coincidences are observed, while a 0 indicates that coincidences were sought and definitely not observed. Experiments that were not done

are shown as · · · in the table. The 0.565-Mev peak was too weak to be seen in either the normal or 0.0574-Mev coincidence spectra, so a question mark is shown.

III. BETA-RAY SPECTRUM

Previous reports[4,5] on the beta spectrum listed only three resolved components, but suggested the probable existence of other lower-energy branches. The newly discovered gamma rays, together with facts about the level scheme deduced from the coincidence measurements, indicated that there must be two more components. A successful attempt to resolve them was made with the magnetic double-focusing spectrometer at the University of Michigan.

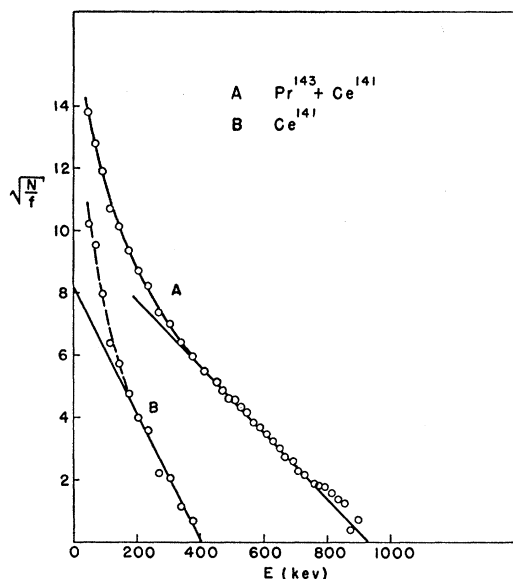Analysis of the spectrum is complicated by the presence of longer lived low-energy components due to

FIG. 4. Kurie plots of residual beta spectrum of Pr¹⁴³ and Ce¹⁴¹ components after decay of Ce¹⁴³. A. Composite spectrum. B. Remainder after subtraction of Pr¹⁴³.

the daughter product Pr¹⁴³ and also Ce¹⁴¹, the latter representing initially about 2% of the activity. The spectrum had to be remeasured after the Ce¹⁴³ had died out, to determine the contributions of these activities to the counting rates in the initial study. Total activity of the sources was followed with an ionization chamber, and the results obtained over a 32-day period indicate half-lives of 33.4 hours and 13.95 days for Ce¹⁴³ and Pr¹⁴³ respectively. The half-life of Ce¹⁴¹ was taken to be the previously reported[6] 33.1 days, which was not verified here.

The source, which had been irradiated for 37 hours, was mounted on a narrow strip of cellulose tape. The G-M counter was equipped with a Zapon window about 15 micrograms per square centimeter in thickness. The initial run of the spectrum was begun about 24 hours after the end of the irradiation, and covered a period of
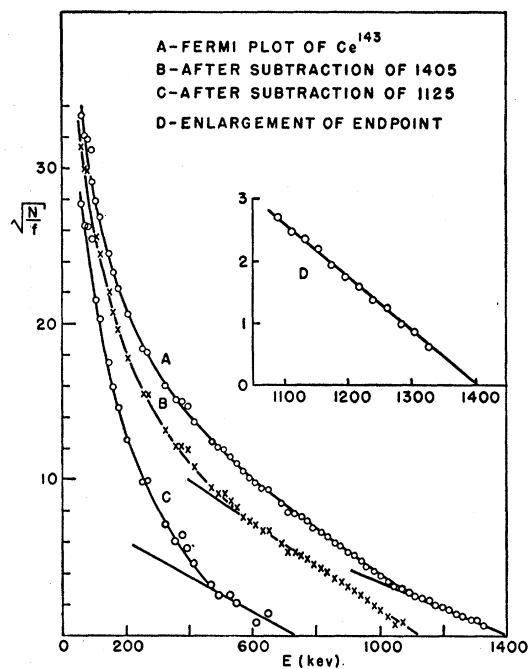
FIG. 5. Kurie plots of Ce¹⁴³ beta spectrum. A. Total composite spectrum. B. Remainder after subtraction of 1.40-Mev component. C. Remainder after further subtraction of 1.125-Mev component. D. Enlargement of end-point region of A.

three days. The second run was begun seventeen days later, and required thirteen days to complete because of the very low counting rates.

In order to make proper corrections for the long-lived components, the residual composite spectrum of the second run was resolved into its Pr¹⁴³ and Ce¹⁴¹ components. A Kurie plot using the Fermi functions and half-life characteristic of the Pr¹⁴³ decay yields a straight line with an end point of 0.93 ± 0.01 Mev for the highest-energy component (see Fig. 4). The Kurie plot for the remainder, using the Fermi functions and half-life for Ce¹⁴¹, is also shown in Fig. 4. Although the plot suggests only a single component (except for considerable upward deviation below 150 kev), the data are not inconsistent with the reported[6] two components of Ce¹⁴¹. They are not resolved here because of the very low counting rates associated with this activity in the source.

The Pr¹⁴³ and Ce¹⁴¹ spectra were corrected for decay and subtracted from the original data of the first run, after which the remainder was corrected for the 33.4-hr decay of Ce¹⁴³. The Kurie plot is shown in Fig. 5 with the numerous internal-conversion lines at low energies omitted.

In analysis of this complex Kurie plot, an allowed shape is assumed for all components. This is consistent with the log ft values eventually determined, and with the appearance of each component in the plot. However, only the high-energy end of each one is seen because of the complexity of the spectrum. All straight-line fits are made by the method of least squares. The plot is re-
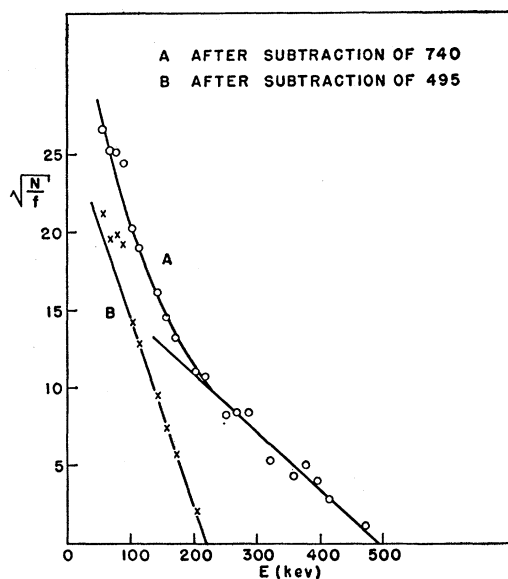
FIG. 6. Kurie plots of the two lowest energy beta components of Ce[143]. *A.* Remainder after subtraction of 1.40-, 1.125-, and 0.74-Mev components. *B.* Remainder after further subtraction of 0.50-Mev component.

solved into five components, as shown in Figs. 5 and 6 and listed in Table III. After subtraction of the first two components, the plot was a little ambiguous, and further analysis is based in part on independent information that there is a component of around 0.7 Mev in coincidence with gamma radiation (see below). The fact that

points below 0.1 Mev still lie somewhat above the last straight line can probably be attributed to backscattering in the source. The errors quoted in Table III represent the statistical uncertainties in the least-squares fit. In the case of the lowest-energy component, the calculated statistical error was very small and was not believed to be significant after so many subtractions.

A semiquantitative measurement of the beta rays in coincidence with various gamma rays was made with the scintillation spectrometer. The beta rays were detected with an anthracene crystal $\frac{3}{16}$ inch thick and $1\frac{1}{2}$ inches in diameter, coupled to an RCA 5819 photomultiplier. The pulse spectrum was examined with the ten-channel analyzer, gated by a NaI(Tl) gamma-ray counter and single-channel analyzer. The source, on a cellulose tape backing, was placed between the two closely spaced counters and 900 mg/cm^2 of Al covered the gamma counter as a beta shield. An Al foil of about 5 mg/cm^2 thickness covered the beta counter as a light shield.

An energy calibration and an indication of the performance of the spectrometer were obtained by examining the beta spectrum and the conversion line of Cs[137], shown in the insert on Fig. 7. The beta spectrum is seen to display a rather long straight section that extrapolates to zero at approximately the expected end point, despite the fact that the curve trails off far beyond this end point. It appears from this, and is consistent with other experience, that spectra from this counter can give rough estimates of end-point energies without correction for resolution, scattering, etc. No attempt is made to deduce Kurie plots from these data.
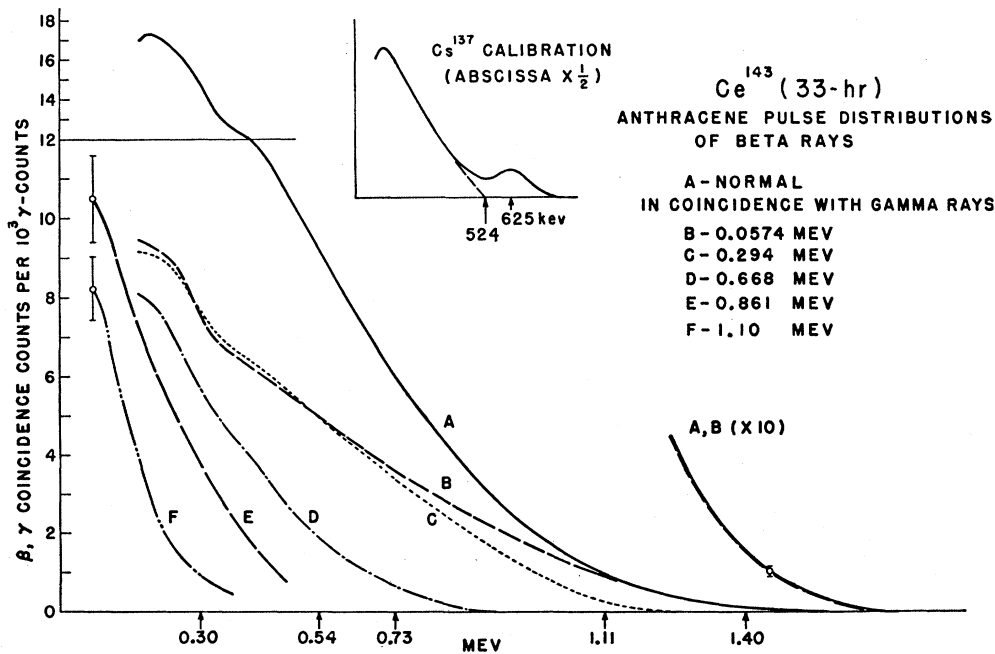

FIG. 7. Anthracene pulse-height distributions of the beta rays of Ce[143]. *A.* Normal or ungated spectrum. *B–F.* Coincidence spectra gated by gamma-ray pulses of energies: *B.* 0.0574 Mev; *C.* 0.294 Mev; *D.* 0.668 Mev; *E.* 0.861 Mev; *F.* 1.10 Mev. Insert shows the spectrum of Cs[137] in the same geometry (abscissa×$\frac{1}{2}$). All curves normalized as coincidence counts per gamma count.

Curve A of Fig. 7 is the ungated scintillation beta spectrum of Ce¹⁴³, while curves B, C, D, E, and F are the spectra in coincidence with the gamma-ray peaks of 0.0574, 0.294, 0.668, 0.861, and 1.10 Mev, respectively. The arrows indicating end points are placed in accordance with the Cs¹³⁷ calibration. For the first three components, the indicated end point is at the energy determined by the magnetic spectrometer measurements, while for the last two they are placed at somewhat higher energies as expected from the gamma-ray energies.

It is evident that there really are five distinct components, and that each is consistent (within the very considerable uncertainties) with one of the expected end points and the above extrapolation criterion. The disagreement in the energies of the two lowest-energy components between the magnetic spectrometer measurements and the gamma-ray measurements cannot be resolved from the scintillation spectra. Counting statistics are indicated for a few representative points in Fig. 7, and are seen to be very poor for the low-energy components despite counting times of several hours.

Each component is seen without the presence of any higher energy components so that no subtractions were

FIG. 8. The decay scheme of Ce¹⁴³ (33.4-hr).

TABLE III. Summary of the magnetic spectrometer measurements of the beta rays.

Isotope	Beta-energy (Mev)	Intensity (%)	Log ft	Spin change	Parity change
Ce¹⁴³	1.40 ±0.02	37	7.75	0,1	yes
Ce¹⁴³	1.125±0.015	40	7.30	0,1	yes
Ce¹⁴³	0.74 ±0.15	5	7.7	0,1	yes
Ce¹⁴³	0.50 ±0.03	12	6.6	0,1	yes
Ce¹⁴³	∼0.22	6	5.8	0,1	yes or no
Pr¹⁴³	0.93 ±0.01	100	7.60	0,1	yes

required. This is due to the very fortunate circumstance that if a given beta ray and gamma ray are in coincidence, all higher-energy beta rays are coincident only with lower energy gamma rays. Some slight gamma-gamma background is indicated in the last two curves, E and F, but is entirely negligible in all the others.

The normal and 0.0574-Mev coincidence distributions (Curves A and B) merge together above the end of the next lower component (Curve C). Careful examination of this region of the spectrum with good statistics shows no detectable differences. The 1.40-Mev component evidently proceeds to the 0.0574-Mev level, and it can be asserted that there is no slightly higher energy branching to the ground state of intensity more than a few percent of the 1.40-Mev branch.

In one further coincidence experiment, the gamma-ray spectrometer was gated by the beta counter. The behavior of various gamma-ray peaks was observed as the coincident beta rays were attenuated with aluminum absorbers. In every case the coincidence rates were observed to fall off with half-thicknesses of Al consistent with other measurements of the beta-ray energies. Of
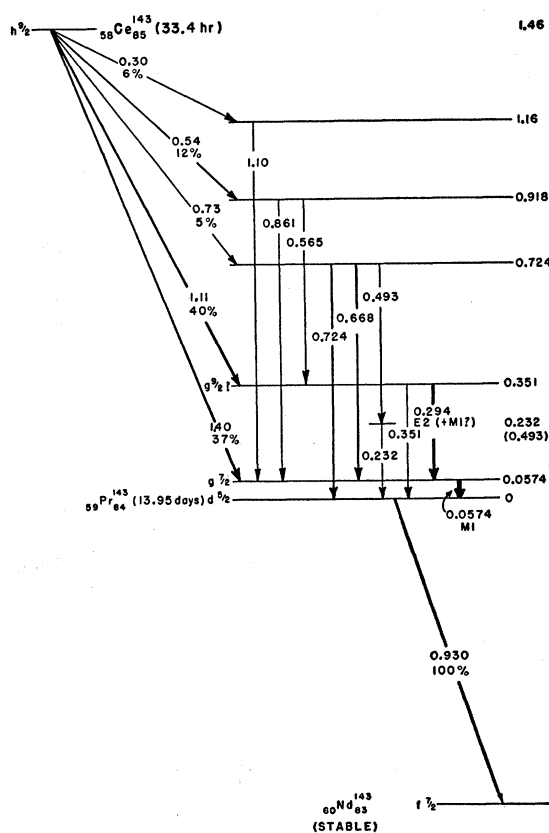
particular interest were the not-fully-resolved gamma-ray pairs 0.294–0.351 and 0.668–0.722 Mev. In each case the compound peak was observed to absorb out without change of shape, indicating that its two component gamma rays originate from the same level.

IV. CONCLUSION

The given data all support the decay scheme shown in Fig. 8. There is some inconsistency concerning the energy of the lowest energy beta-ray component, in that the gamma-ray energies require that the beta ray have an energy of 0.30 Mev, while the magnetic spectrometer analysis indicated a value of 0.22 Mev. The discrepancy is not regarded as serious since the accumulated errors of the many subtractions in the latter analysis must be very considerable. The energy of the 1.10-Mev gamma ray, on the other hand, was measured with reference to the 1.17-Mev line of Co⁶⁰, and is believed to lie within the quoted uncertainty.

The relative order of the 0.493–0.232 Mev cascade was not determined in this study. The excellent agreement of this energy sum with the 0.722-Mev gamma ray leaves little doubt that the cascade does come from this level, however. No other position would be consistent with the gamma-gamma coincidence data.

The value of the K-conversion coefficient (5.9), the predominance of the L_I subshell line in the L-conversion,

and the lifetime (less than the resolving time of the coincidence circuit, 2×10^{-6} second) of the 0.0574-Mev transition are all consistent with an $M1$ interpretation. Lack of exact theoretical values for α_K does not permit exclusion of some $E2$ admixture, but the lack of an observable L_{II} conversion line limits this possibility to a few percent.

The measured K/L ratio of the 0.294-Mev transition indicates several possibilities. $M3$ can be excluded because the life of this state is also less than the resolving time of the coincidence circuit. $M2$ or $E1$ interpretations are inconsistent with the plus parity of the 0.351-Mev state indicated by the beta-ray measurements. The remaining choice is $E2$.

According to the single-particle model, the ground state of Pr^{143} (59 neutrons) may be $d_{5/2}$ or $g_{7/2}$. Either assignment is consistent with the observed character of the beta transition to Nd^{143}, which has a measured spin[6] of 7/2 and is $f_{7/2}$ (83 neutrons). The ground state of Ce^{143} (85 neutrons) may be $f_{7/2}$ or $h_{9/2}$. The $f_{7/2}$ assignment is unsatisfactory since the state could then

undergo a first-forbidden beta transition equally well to either of the possible choices for the ground state of Pr^{143}, whereas the ground-state transition is not observed. If it were $h_{9/2}$, however, decay to a $g_{7/2}$ state in Pr is only first forbidden, but decay to a $d_{5/2}$ state is "l-forbidden" with $\Delta l=3$. This assignment is therefore consistent with observation, if the Pr^{143} ground state is identified as $d_{5/2}$. Then the 0.0574-Mev excited level can be $g_{7/2}$, consistent with the $M1$ character of the gamma transition.

Although it is indicated above that the 0.294-Mev transition appears to be $E2$, the fact that the 0.351-Mev crossover is seen makes it seem unlikely that the 0.351-Mev level has a spin as great as 11/2. It is tentatively suggested that this is a $g_{9/2}$ state, and that there may be some $M1$ admixture in the 0.294-Mev transition.

V. ACKNOWLEDGMENTS

Magnetic Spectrograph Measurements on the $\text{Al}^{27}(d,p)\text{Al}^{28}$ Reaction*

W. W. Buechner, M. Mazari,† and A. Sperduto
Physics Department and Laboratory for Nuclear Science, Massachusetts Institute of Technology, Cambridge, Massachusetts
(Received July 12, 1955)

A broad-range magnetic spectrograph has been used to study the proton groups from $\text{Al}^{27}(d,p)\text{Al}^{28}$. In the region of excitation between the ground state and the neutron binding in Al^{28}, one hundred well-resolved groups were observed and assigned to this reaction on the basis of studies at bombarding energies of 6 and 7 Mev and at several angles of observation. The energy resolution of the proton groups ranged from 800 to 1600.

I. INTRODUCTION

ONE of the most active fields in present nuclear research is the investigation of the excited states of nuclei. An important method for such investigations is the study of the charged particles emitted from artificially produced nuclear reactions. The requirements for resolution and accuracy in this field are such that these studies are now commonly carried out with magnetic or electrostatic deflection of both the bombarding and the emitted particles.

In general, the magnetic or electric analyzers used can be classed as spectrometers, since they focus the charged particles onto a slit and electrical detection is used. A high-resolution study of a particle spectrum with such a spectrometer requires a point-by-point study of the number of particles through a narrow slit

as a function of field strength. In a few cases, magnetic analyzers have been constructed with a geometry such that photographic detection can be employed to record a portion of the spectrum of charged particles. Such a magnetic spectrograph has been in use in this Laboratory for a number of years. While the resolution and accuracy of this instrument have been satisfactory, it has been apparent that an analyzer more closely resembling an optical spectrograph would have many advantages. With such an instrument, which would record simultaneously a considerable fraction of the complete particle spectrum, uncertainties in the energies and relative intensities of the particle groups, which often arise because of target changes during long bombardments, would be considerably reduced. Also, in cases where the spectrum to be investigated consists of more than a few groups, the resolution which could be obtained in practice with such a spectrograph would be greater than would be practical with the more usual spectrometer instrument.